STUDIA UNIVERSITATIS BABEŞ-BOLYAI, CHEMIA, XLII, 1-2, 1998

NUMERICAL SIMULATION OF A PRESSURE SWING ADSORPTION UNIT

THOMAS KLEINHEMPEL, MARIETA ATANASIU, FLORIN ATANASIU*

ABSTRACT. The paper presents a numerical model that simulates the bulk separation of a two component gas mixture, on 5 A molecular sieve. Experimental results are compared with theoretical ones, to reveal the influence of some operating parameters on the product purity and recovery. Experiments have been carried out for air separation on 5 A zeolite molecular sieve on a two column laboratory PSA unit. The theoretical model provides a good representation of the performances of an experimental unit over the range of operating conditions.

INTRODUCTION

SKARSTROM [1] presents in 1960 "a new method for air drying" for the first time, based on selective adsorption process that is called ***"heatless adsorption"*** or ***"pressure swing adsorption"*** at the present time. The process consists in a cyclic operation of two adsorption columns between two limiting pressures: a low one (p_L) and a high one (p_H). The standard operational cycle consists in four steps: pressurization with feed from the pressure p_L up to p_H, constant pressure production (adsorption) step at p_H, followed by blowdown from p_H down to p_L and constant pressure purge at p_L with a fraction of the purified product, withdrawn during the production step. The bulk separation of the feed mixture is processed during pressurization and production steps. The bed regeneration is accomplished by reducing the partial pressure of the more strongly adsorbed component during blowdown step, when the total pressure decreases and then by purging the adsorption bed with purified gas, when the molar fraction of the stronger adsorbed components is reduced on the adsorbent surface.

Beginning with 1970, the process was widely used for various gas separations [2], on laboratory units, as well as on industrial plants, by experimenting other operating cycles, other adsorbents like zeolites and – during the last decade - carbon molecular sieves. Thus the PSA technology has been extended from drying of the gases to air separation, in order to obtain pure oxygen and/or nitrogen, air purification, hydrogen and helium separation, by retaining impurities such as CO_2, H_2O, H_2S, NO_2, SO_2, NH_3 and CH_4.

* *S.C. "GAS" S.R.L. Societate Comercială pentru Gaze şi Aparatură, Cluj-Napoca.*

Together with technology development, the numerical modeling of the process gained greater attention, for plant design as well as for simulation, in order to find the best sets of values for the operating conditions.

This paper presents a local equilibrium model for the simulation of a two-bed PSA unit operation, based on the standard four-step cycle presented above. The model consists in integral molar balance equations, considered between the initial and final moments of each step. The computed results exhibit a good agreement with the experimental ones. A parametric study was also accomplished, in order to reveal the influence of the purge velocity and the product velocity on the purity and the recovery fraction of the product.

THEORETICAL MODEL

A two-bed process operated on a standard cycle is considered, as shown in fig.1. The pressure changes in the adsorption bed during a whole cycle are presented in figure 2.The following four steps comprise the cycle:

1) Pressurization,
2) Adsorption,
3) Countercurrent blowdown,
4) Countercurrent purge.

In step 1, bed 1 is pressurized to the high operating pressure with feed and bed 2 is blown down to the atmospheric pressure in the reverse flow direction. In step 2, the high pressure feed flow trough bed 1. During this step the more strongly adsorbed component is retained in the bed and the interstitial gas stream is enriched in the lighter component, that leaves as effluent. A fraction of the effluent stream is

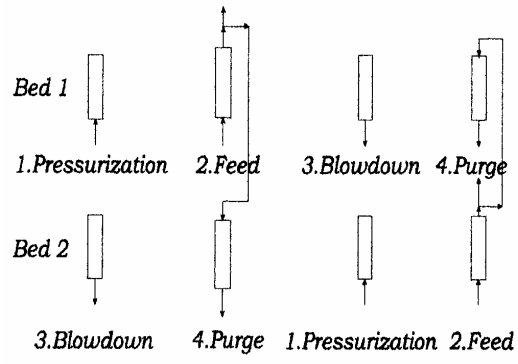

Fig.1. Schematic diagram of the P.S.A. cycle

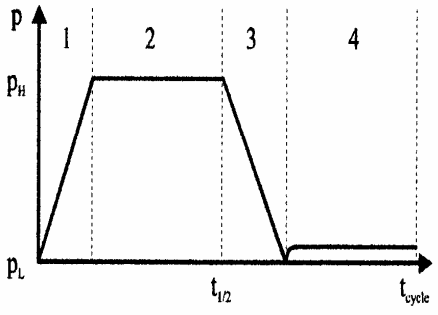

Fig. 2. Pressure changes in the bed during a whole cycle

withdrawn as product and the rest is used for countercurrent purge of bed 2 at reduced pressure. The operations are switched between beds in steps 3 and 4.

In order to develop the mathematical model for this system, the following assumptions are introduced:

1) Air is considered as a binary mixture of ideal gases 78% nitrogen (1) and 22% oxygen together with argon (2). Because argon exhibits almost the same adsorption affinity for 5A zeolite molecular sieve (ZMS-5A) as oxygen in the range of ambient temperatures, these two components are considered unseparated. They are enriched in the raffinate product.

2) Local equilibrium is assumed. The mass transfer between gas and solid phase is considered to be instantaneous.

3) The system is assumed to be isothermal. When small diameter columns are used, with high thermal conductivity, as in the present study, the pressure flow direction is changed frequently and the heat evolved during adsorption does not exceed 5 kcal/mol, thermal effects can be neglected.

4) Equilibrium relationships for both components are represented by binary LANGMUIR isotherms.

5) Pressure drop along the column is neglected.

6) Repressurization is carried out only with feed mixture.

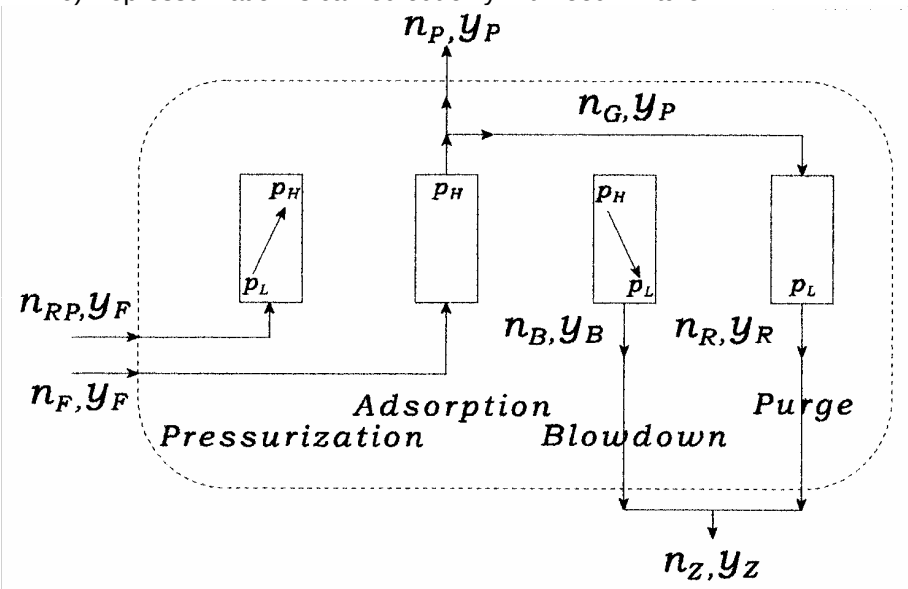

Fig.3. Schematic diagram of the molar balance

The molar balance equations are written for the entire stream and for the most strongly adsorbed component, in this case – nitrogen, between the initial and the final moment of each PSA step. Figure 3 shows the schematic diagram used to complete the balance and the meaning of the symbols.

Starting from an initial equilibrium state of the bed with feed mixture (air) at the pressure p_L and the average concentration y^o_4 of the nitrogen in the interstitial gas phase, the adsorbent is put in contact with the feed during the pressurization step. The pressure raises to p_H and the average concentration of the interstitial gas phase changes to y_1 due to the incipient adsorption. The average mole number of

gas fed in the column during pressurization is n_{RP}. Then, the column is feed with n_F moles of air in the adsorption step, the pressure remain unchanged at p_H and the composition become y_2 at the end of the step.

Table 1.

The state of the bed at the beginning and end of each PSA step.

P.S.A. step	PRESSURIZATION	ADSORPTION	BLOWDOWN	PURGE
Initial state of the bed	p_L, y_4	p_H, y_1	p_H, y_2	p_L, y_3
Final state of the bed	p_H, y_1	p_H, y_2	p_L, y_3	p_L, y_4

From the column (n_P+n_G) moles of oxygen enriched gas are extracted, the average gas phase composition being y_P. One fraction represents the useful product (n_P) and the other one is used to regenerate the neighbor column during the purge step. In the blowdown step the pressure decreases to p_L, n_B moles of gas are vented with the average composition y_B and the column remain in equilibrium with an interstitial gas phase with y_3 average nitrogen concentration. During the final step of the cycle, the pressure remain unchanged at p_L, n_G moles of oxygen enriched gas are fed at the outlet end of the column and n_R moles of gas with the average concentration y_R are vented at the inlet end of the column. At the end of the step, the bed remains in equilibrium with an interstitial gas having y_4 nitrogen concentration. Starting from the remaining y_4 equilibrium composition, this computation algorithm is continuing until the product composition reaches a constant value. At this moment the PSA unit has reached its steady state functioning.

The time duration of adsorption and purge steps is t_1 and of pressurization and blowdown is t_2. By combining the two vented gas fractions from blowdown and purge, a resulting "residue" can be obtained, having n_Z number of moles and y_Z average nitrogen mole fraction.

Subject to these considerations, the system of governing equations describing the cyclic operation is presented below.

Pressurization step (1):

Overall molar balance:

$$n_{RP} + [m_s.W^*_{1+2}(p_L,y_4) + N_{g,L}] = [m_s.W^*_{1+2}(p_H,y_1) + N_{g,H}] \quad (1)$$

Partial molar balance, made on the component 1 (nitrogen):

$$n_{RP}.y_F + [m_s.W^*_1(p_L,y_4) + y_4.N_{g,L}] = [m_s.W^*_1(p_H,y_1) + y_1.N_{g,H}] \quad (2)$$

Isobaric production step (2):

Overall molar balance:

$$n_F + [m_s.W^*_{1+2}(p_H,y_1) + N_{g,H}] = (n_P+n_G) + [m_s.W^*_{1+2}(p_H,y_2)+N_{g,H}] \quad (3)$$

Partial molar balance, made on the component 1 (nitrogen):

$$n_F.y_F + [m_s.W^*_1(p_H,y_1) + y_1.N_{g,H}] = (n_P+n_G).y_P + [m_s.W^*_1(p_H,y_2)+y_2.N_{g,H}] \quad (4)$$

Blowdown step (3):

Overall molar balance:

$$[m_s.W^*_{1+2}(p_H,y_2) + N_{g,H}] = n_B + [m_s.W^*_{1+2}(p_L,y_3) + N_{g,L}] \quad (5)$$

Partial molar balance, made on the component 1 (nitrogen):

$$[m_1.W^*_1(p_H,y_2) + y_2.N_{g,H}] = y_B.n_B + [m_s.W^*_1(p_L,y_3) + y_3.N_{g,L}] \quad (6)$$

Isobaric purge step (4):

Overall molar balance:

$$n_G + [m_s.W^*_{1+2}(p_L,y_3) + N_{g,L}] = n_R + [m_s.W^*_{1+2}(p_L,y_4) + N_{g,L}] \quad (7)$$

Partial molar balance, made on the component 1 (nitrogen):

$$n_G.y_P + [m_s.W^*_1(p_L,y_3) + y_3.N_{g,L}] = n_R.y_R + [m_s.W^*_1(p_L,y_4) + y_4.N_{g,L}] \quad (8)$$

where: $N_{g,H} = p_H.\varepsilon.A.H/(R.T)$ and $N_{g,L} = p_L.\ \varepsilon.A.H/(R.T)$

The volumetric purge-to-feed ratio (the reflux ratio) represents the ratio between the volume of purge gas V_G and feed gas V_F. The purge gas is extracted from the high purity product and recirculated in the bed at p_L during the purge step, countercurrently with the feed. The feed gas volume is considered at high pressure. The value of γ is equal to the molar ratio multiplied with the pressure ratio, as shown in equation (9).

$$\gamma = \frac{V_G(p_L)}{V_F(p_H)} = \frac{n_G}{n_F} \cdot \frac{p_H}{p_L} \quad (9)$$

The equilibrium isotherms, together with a van't HOFF type of temperature dependence, can be either linear or LANGMUIR type (i=1,2).

- linear: $W_i^* = K_i.p.y_i = W_i^*(p,y_i,T)$ (10)

$K_i = K_{oi}.\exp[q_i/(R'.T)]$ (11)

- binary LANGMUIR type:

$$W_i^* = \frac{m_i \cdot b_i(T) \cdot p \cdot y_i}{1 + b_1(T) \cdot p \cdot y_1 + b_2(T) \cdot p \cdot y_2} = W_i^*(p, y_i, T) \quad (12)$$

$b_i = c_i.\exp[q_i/(R'.T)] = b_i(T)$ (13)

The linear equations describe correctly the adsorption equilibrium of nitrogen and oxygen on 5A - ZMS only in the range of small partial pressures (up to 1 atm). Because the operation of the unit is carried out under super-atmospheric pressures, the binary LANGMUIR equation is preferred. It correlates correctly the experimental gas-solid equilibrium data on the entire range of partial pressures.

As initial conditions, the bed is considered to be in equilibrium with air, at the low pressure of the system. There is no flow trough the column.

$$y_{(t=0)} = y^o_4 = y_F; \qquad q_{(t=0)} = 0; \quad (14)$$

The average mole numbers is converted to average flow rates by using the equation of state of the ideal gases and the duration of each step of the cycle. For the isobaric steps we have:

$$G^o_{V,F} = n_F.R.T^o/(t_1.p^o), \quad G^o_{V,G} = n_G.R.T^o/(t_1.p^o), \quad G^o_{V,P} = n_P.R.T^o/(t_1.p^o) \quad (15)$$

and for the non-isobaric steps:

$$G^o_{V,RP} = n_{RP}.R.T^o/(t_2.p^o), \quad G^o_{V,B} = n_B.R.T^o/(t_2.p^o) \quad (16)$$

The model was numerically solved by NEWTON's method, applied to the systems of non-linear equation [3]. As known parameters are considered: the flow rate and the composition of the feed, the diameter and the height of the adsorption bed. There are also considered the volumetric purge-to-feed ratio (γ), the ambient temperature (T), the limiting pressures (p_H and p_L), the steps' duration t_1 and t_2, the porosity and bulk density of the adsorbent bed, equilibrium parameters. As unknown parameters, the model calculates the average flow rates and compositions of production, blowdown, purge inlet and purge outlet streams and the average composition of the interstitial gas at the end of each step. In order to obtain a unique solution for the governing system we used the following assumption: the column is operated up to very close to the breakthrough moment. That means, in the view of the local equilibrium theory that the whole adsorbent is in equilibrium with the feed gas at the end of the production step. The mathematical reflection of this assumption is equation (17):

$$y_2 = y_F \tag{17}$$

By assuming local equilibrium, the length of the mass transfer zone is neglected. So, at the breakthrough moment of the most strongly adsorbed component in the purified product, the entire bed is in equilibrium with the feed mixture. In reality, the length of the mass transfer zone cannot be neglected. The length of the mass transfer zone is significant in bulk separation, when there are more then one adsorbed component in the feed, with significantly high concentration. This is the case of oxygen/nitrogen separation on 5A –ZMS. At the breakthrough moment it's presence determines the existence of a quantity of adsorbent material that can separate new quantities of feed, amount that will not be used. From this point of view the use of a so-called "dynamic adsorption capacity", instead of the equilibrium adsorption capacity, will approach the simulated results to the experimental ones.

From the experimental breakthrough curves of the authors [12], with the help of the algorithm presented by TARAN [5], it has been estimated that the experimentally used adsorbent exhibits only 65-75% of its equilibrium adsorption capacity, in dynamic conditions. This value depends on the operating conditions, but an average value of 71% can be considered for our purpose. So, the simulations have been carried out with a correction factor of 0.71 to multiply the adsorption capacity computed from LANGMUIR type equations.

The residual wasted gas extracted from the PSA unit and collected both during blowdown and purge steps, is enriched in nitrogen and it's concentration is somewhat greater than in the feed air. The mean value of this can be computed by using the equation (18).

$$y_Z = \frac{n_B \cdot y_B + n_R \cdot y_R}{n_B + n_R} \tag{18}$$

Based on the above equations, the authors developed a computation program by using the Pascal language.

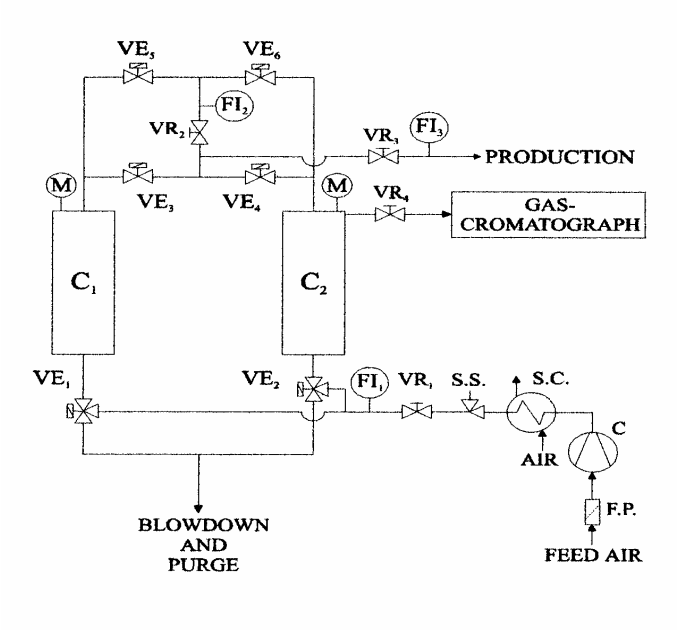

Fig. 4. The experimental PSA unit

EXPERIMENTAL

The experimental PSA unit used is shown in figure 4. It consists in two adsorption columns C_1 and C_2, six solenoid valves to lead the gas streams in order to accomplish the four steps of the cycle. There are also three flow indicators FI_1-FI_3, with the appending regulating valves, in order to measure and regulate the flow rates of feed, purge and production. Two pressure gauges M indicates the pressure at the top of the columns and the regulating valve VR_4 extract samples to the gas chromatograph coupled with a thermal conductivity detector. The compressor C feeds Air is passed trough the dust filter FP, compressed in the compressor C and cooled to atmospheric temperature in the SC cooler. The safety valve SS leads to the atmosphere the exceeding compressed air.

The dimensions and other details of the unit together with the equilibrium parameters are summarized in table 2.

Table 2.

The main parameters of the experimental PSA unit.

Adsorbent:		5A-ZMS
Adsorption bed length:	H [m]	0,51
Internal diameter of the column:	D_i [m]	0,074
Diameter of adsorbent particle:	d_p [mm]	1-2
Adsorbent porosity:	ε [/]	0,4
Bulk density of the adsorption bed:	ρ_s [kg/m^3]	772
Ambient temperature:	T [^{o}C]	20

Low pressure:	p_L [atm]	1
High pressure:	p_H [atm]	3,2
Feed flow rate:	F [Nl/min]	14-45
Production flow rate:	P [Nl/min]	0,5-3
Feed composition:		22% (oxygen + argon), 78% nitrogen
LANGMUIR parameters:		
Saturation adsorption capacity:	m_1 (N_2) [kmol/kg]	2,217.10-3
Saturation adsorption capacity:	m_2 (O_2) [kmol/kg]	3,120.10-3
Saturation adsorption capacity:	m_3 (Ar) [kmol/kg]	3,966.10-3
Pre-exponential factor:	c_1 (N_2) [atm^{-1}]	4,459.10-5
Pre-exponential factor:	c_2 (O_2) [atm^{-1}]	13,53.10-5
Pre-exponential factor:	c_3 (Ar) [atm^{-1}]	11,078.10-5
Isosteric heat of adsorption:	q_1 (N_2) [kcal/kmol]	4880
Isosteric heat of adsorption:	q_2 (O_2) [kcal/kmol]	3325
Isosteric heat of adsorption:	q_3 (Ar) [kcal/kmol]	3248

The adsorption isotherms for oxygen, nitrogen and argon on commercial 5A ZMS have been obtained at 20^{o}C, by using a volumetric method. It was fount out that the experimental values were very close to those reported by VERELST and BARON [6], so there were used the LANGMUIR parameters reported in [6].

RESULTS AND DISCUSSION

The program have been tested by using, first a set of experimental data published by FAROOQ and RUTHVEN [7] and then with a few sets of experimental data obtained on the PSA unit presented schematically in fig.4. The experimental and simulated data are presented in Table 3. In both situations the relative errors of computed oxygen purity, recovery and flow rate lied between 0.4-5%, as the experiment can be more or less approximated by the model.

In computation, we have used the dynamic adsorption capacity, instead of the equilibrium values, as we have been explained above. This takes somehow account for the finite mass transfer velocity and axial dispersion of the gas and allows a good prediction for the experimental values.

Starting from the equilibrium state of the adsorbent with air, to achieve the maximum purity of oxygen (96% O_2) the equipment needs 20-30 experimental cycles, while simulation needs only 2-6 full cycles, depending on the purge ratio. This difference has both experimental and modeling causes. The retention of humidity (2-3% v/v) and carbon dioxide (300-600 ppm) from the ambient air, both with high adsorption affinity for 5A-ZMS, follows the same cycle as the useful nitrogen-oxygen separation. So the oxygen-enriched stream is completely dry and CO_2 free (max 2 ppm humidity and max 1 ppm CO_2). A part of the bed works to accomplish that during pressurization and production steps, but this part needs also to be regenerated with the purge stream. This behavior delays a little the experimental unit to reach the steady state conditions. The mathematical model does not account for the presence of humidity and CO_2. Furthermore, to obtain compatibility for the equations' system we considered the bed operated close to the breakthrough point. These assumptions may reduce the simulated transient period time.

An important parameter that evaluates the performances of any separation equipment is the ***recovery*** fraction of the useful product from the feed. For our case it is defined [4,7,8] to be the ratio of the moles of oxygen from the main product and the moles of oxygen from the feed.

$$R_C = \frac{P \cdot y_P}{F \cdot y_F} \tag{19}$$

Table 3 presents the main experimental results compared to the simulated ones. The table covers a large range of the production composition, between 40-95% oxygen purity. We have obtained a good correlation between experimental and simulated results, especially for oxygen purity above 90%.

Table 3.

Experimental and simulated results for oxygen/nitrogen separation.

Run	F [l/kg/cycle]	PG [l/kg/cycle]	PR [l/kg/cycle]		O_2 Purity [%]		O_2 Recovery [%]	
			Exp.	Calc.	Exp.	Calc.	Exp.	Calc.
1	0,6872	0,4270	0,0809	0,0828	86,35	86,26	48,41	49,21
2	0,6536	0,4371	0,0453	0,0448	92,63	92,84	30,60	30,15
3	0,7459	0,4491	0,096	0,0974	77,45	86,32	47,77	53,34
4	0,7794	0,4251	0,1223	0,1230	71,52	86,60	53,42	64,73
5	0,7375	0,4152	0,0096	0,0101	94,61	96,00	5,86	6,23
6	0,8530	0,0253	0,0083	0,0108	70,08	68,20	53,95	68,5
7	0,6360	0,4251	0,0646	0,0498	89,34	88,42	43,18	32,75
8	1,1150	0,4626	0,0453	0,0446	88,48	94,20	17,20	17,83
9	0,5765	0,3260	0,0453	0,0457	91,89	93,20	34,38	35,14
10	0,4286	0,2741	0,0483	0,0550	67,08	67,60	35,12	41,17
11	0,3576	0,1720	0,0483	0,0512	44,35	46,47	28,55	31,69

The studied PSA configuration does not exhibit high recoveries, its' values do not exceeding 30% for oxygen purity over 90%. Even if the feed air is cheep, the major operating cost is supported by the compression energy. So the rather low recovery decreases the efficiency of the compression energy's expense. A raise of the recovery can be accomplished only with a significant decrease of the purity, for this PSA configuration. In order to obtain higher recoveries together with high purity of the enriched product, other configurations have been imagined [2], which use vacuum or intermediate pressurization steps, for oxygen separation, or even combination with other separation procedures, like in the case of helium separation [8,9].

The influence of the purge flow rate on the purity and the recovery of oxygen have been studied. The results are presented in figure 6 and 7. We have also studied the influence of the purge-to-feed ratio on the transient behavior of the PSA unit. The results are shown in figure 5.

From equation (9) we can find that a value of $\gamma = 0$ represents the zero reflux situation, when the purity of the product is minimum and the recovery is maximum. This situation is similar to the distillation. In this case the PSA separation occurs only

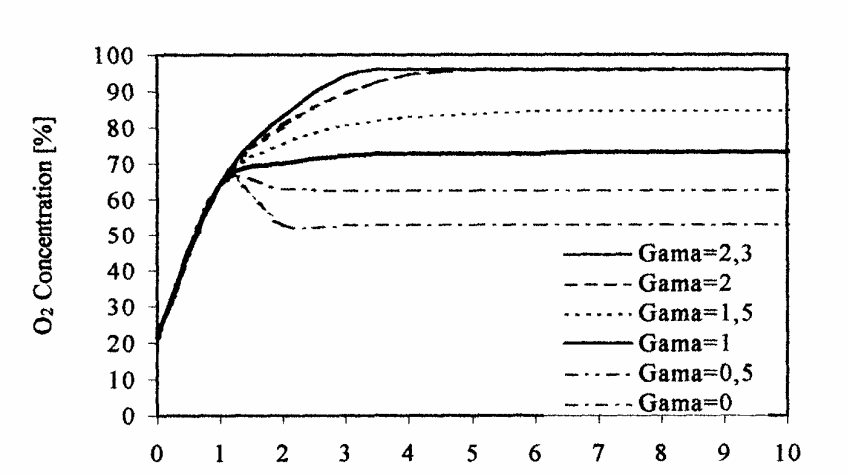

Fig. 5. The influence of the purge-to-feed ratio on the transient behavior

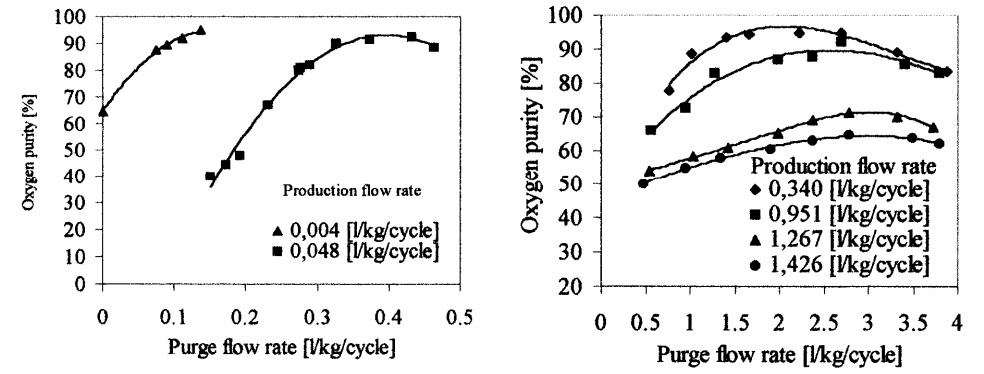

Fig. 6. The influence of the purge flow rate on the oxygen purity

during the pressurization step, when the maximum oxygen purity does not exceed 50-60%. That depends on the pressurization velocity, high and low pressure ratio, production flow rate, equilibrium and kinetic particularization. Figure 5 also shows the existence of a minimum value of the purge ratio γ =1 that allows the achievement of a high purity product. In practice γ >1 is required. For higher values of γ, the higher is the necessary feed rate – for a given product rate, the higher is the separation effort of the bed and the start-up transient state is longer. This, because the gain of the oxygen purity between two cycles is lower.

Figure 6 shows the influence of the reflux on the oxygen purity, at different values of the production flow rate and figure 7 on the recovery ratio, at different values of the purge flow rate. The solid lines represent simulated results and the dotted lines, the experimental ones. Figure 5 and 6 shows that increasing the purge ratio the purity of the high-pressure product can be increased and figure 7 shows that in these circumstances the recovery of the desired product lowers. The

general trend of the process indicates that for a given production flow rate, the high pressure product purity raises up to a maximum value by raising the purge flow rate and then the purity decreases slowly. The purity gain is achieved by regenerating the bed with a supplementary quantity of purge gas, with higher purity, which is obtained by raising the feed. From a certain value, the separation capacity of the column will be exceeded and the purity of the product will decrease. For each value of the production flow rate will be an optimum value of the purge rate that allows the maximum possible purity.

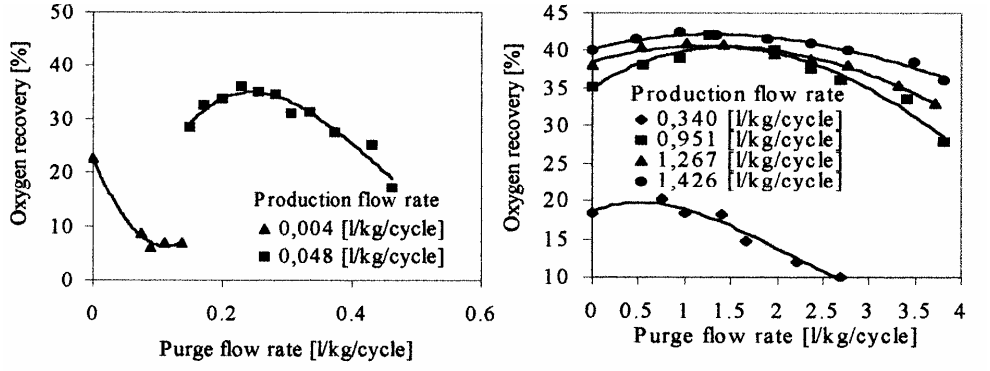

Fig. 7. The influence of the purge flow rate on the oxygen recovery.

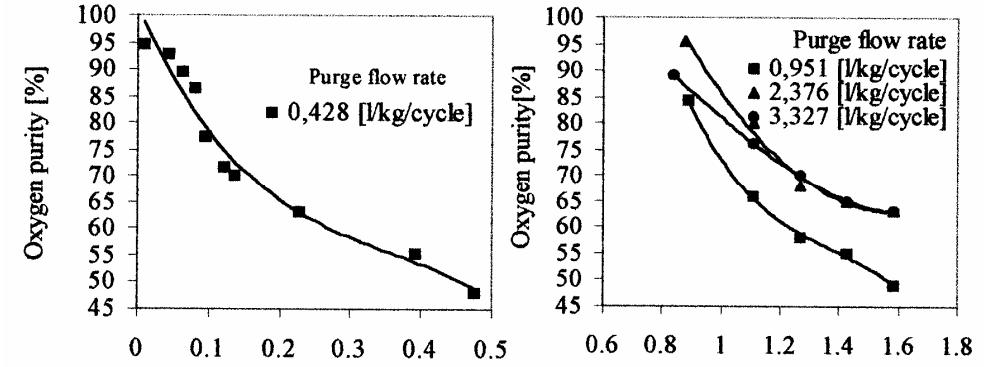

Fig. 8. The influence of the production flow rate on the oxygen purity

The trend of the oxygen recovery generally follows the trend of the purity, as can be seen in figure 7. But if at low production flow rates the recovery raise is due to the raise of the product purity, at higher production flow rates the recovery raise is due to the raise of the production flow rate. We can understand from these figures that, for a given production flow rate, the PSA unit can be operated either at high purity, with the afferent loss of purity, or at high purity, with the resulting recovery fraction, depending on the specific application.

We have also studied the influence of the production flow rate on the purity and recovery of oxygen, for a given purge flow rate. Figure 8 shows that increasing

the production flow rate the purity decreases quite rapidly. The high purity can be regained by further increase of the purge, until the separation capability of the bed starts to be exceeded. For a given value of the purge flow rate, only the raise of the feed can do the raise of the production. This determines some breakthrough of the nitrogen in the high-pressure product that lowers its purity. In any case figures 6 and 8 shows that this PSA configuration can exhibit a production spare of production capacity between 8-50%, with the afferent loss of purity. These are useful in some applications of low concentration oxygen, like water oxygenation, natural gas burning enhancement and other oxidation processes.

Figure 9 presents the influence of the production flow rate on the recovery fraction of the high-pressure product for a given purge flow rate. As the production raises, the recovery raises, despite the decreasing of the oxygen purity. From the figures we can observe that for low purge rates the raise of the recovery is greater then at higher purge rates. As the later one still raise, a new raise of the production determines a smaller raise of the recovery.

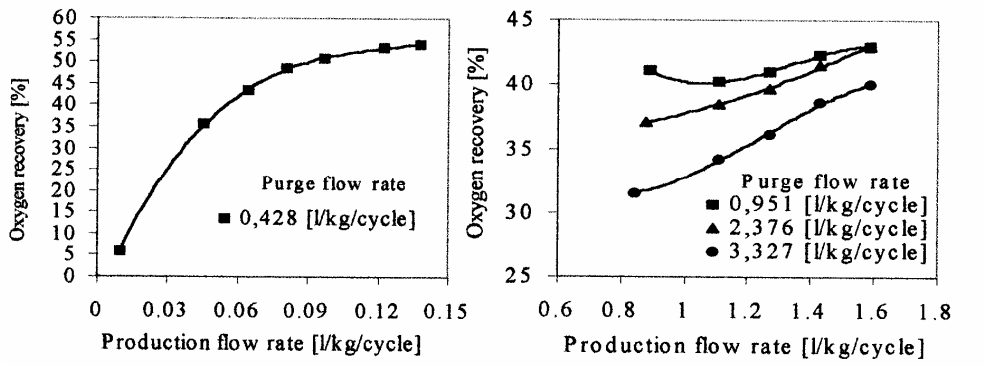

Fig. 9. The influence of the production flow rate on the oxygen purity.

For the studied PSA configuration and for oxygen purity over 90%, we cannot expect recoveries greater then 30-35%, because this purity can be obtained only with a high value of the purge-to-feed ratio, laying between 1.5-2. There have been imagined other configurations [2], by using vacuum steps instead of low pressure purge, different pressurization policies, that involves one or more pressure equalization step and higher number of columns (3 to 5) for a continuous production flow rate. Even with these improvements, the recovery fraction does not exceed about 50-55%, for oxygen concentrations above 90%.

CONCLUSIONS

An equilibrium mathematical model have been developed for the simulation a PSA unit operated with 4 steps/cycle, that separates a binary bulk feed mixture with the adsorption of both components. Based on this model, a numerical program has been carried out.

A laboratory scale PSA unit has been built, with two columns, operated with the above mentioned cycle, that separates air on 5 A zeolite molecular sieve and delivers an oxygen enriched high pressure product. We have been obtained

oxygen purity up to 94%. The experimental values obtained have been compared with the simulated ones and a good agreement has been found between these.

Some parametric studies have been accomplished by using both the experimental unit and the simulation program, in order to stand out the influence of the production and purge flow rates on the high-pressure product purity and recovery fraction. The complexity of the interdependence of the operating parameters has been emphasized. From the above shown figures, we can find the optimum values of the purge flow rate for a given yield.

NOTATION

A = cross section of the bed, m^2
$b_{1,2}$ = gas-solid interaction parameter in Langmuir equation, atm^{-1}
$c_{1,2}$ = pre-exponential parameter in Langmuir equation, atm^{-1}
D_i = internal diameter of the bed, m
F = feed flow rate
G^o_V = volumetric flow rate of the gas flow rate, Nm^3/s
H = height of the bed, m
$m_{1,2}$ = saturation adsorption capacity, kmol/kg
m_s = adsorbent quantity, kg
n = moles of gas
N_{GH} = moles of interstitial gas, at pressure p_H
N_{GL} = moles of interstitial gas, at pressure p_L
p = total pressure, atm
p_H = high pressure of the system, atm
p_L = low pressure of the system, atm
$q_{1,2}$ = isosteric heat of adsorption, in Langmuir equation, kcal/kmol
R = 0,082 m^3.atm/kmol/K, R' = 1,9872 kcal/kmol/K, gas constant
Rc = recovery fraction, %
t_1 =duration of isobaric phases, s
t_2 = duration of non-isobaric phases, s
T = temperature, K
V_F = volume of feed gas, at pressure p_H, m^3
V_G = volume of purge gas, at pressure p_L, m^3
w^o_f = gas velocity in the empty column, Nm/s
$W^*_{1,2}$ = adsorbed quantity, kmol/kg
y = molar fraction of the stronger adsorbed component
γ = volumetric purge-to-feed ratio
ε = porosity of the bed
ρ_s = bulk density of the bed, kg/m^3

REFERENCES

1. Skarstrom, C.W., U.S. Patent, 2 944 627, 1960.
2. Tondeur, D., Wankat, P.C., Sep.Purif.Methods, **14**, 1985, 2, p.157-212.
3. Démidovitch, B., Maron, I., Éléments de calcul numérique, Ed. MIR-Moscova, 1973 p.454.
4. Flores-Fernandez, G., Kenney, C.N., Chem.Eng.Sci., **38**, 1983, 6, p. 827.
5. Taran, C., în *Ingineria prelucrării hidrocarburilor*, vol. 3, cap. 7, Editura Tehnică, Bucureşti, 1987.
6. Verelst, H., Baron, J., *J.Chem.Eng.Data*, **30**, 1985, p. 66-70.
7. Farooq, S., Ruthven, D.M., Boniface, H.A., *Chem.Eng.Sci.*, **44**, 1989, 12, p. 2809.
8. Hasselden, G.G., *Gas.Sep.Purif.*, **4**, 1989, p. 209.
9. Asahara, W., Teneda, K., Tsukenda, M., *Gas Sep.Purif.*, **4**, 1988, p. 204.
10. Kleinhempel, M.T., Atanasiu, F., Literat, L., *Revista de chimie*, **46**, 1995, 8.
11. Kleinhempel, M.T., Atanasiu, M., Atanasiu, F., *Oxygen Enrichment by Pressure Swing Adsorption*, Conferința Națională de Chimie şi Inginerie Chimică, Bucureşti, octombrie 1998.
12. Kleinhempel, M.T., Mihăilescu, G., Atanasiu, M., Atanasiu, F., *Modelarea matematică a curbelor de străpungere pentru separarea oxigenului de azot*, Simpozion Național de Inginerie Chimică, Bucureşti, 1998.
13. Barrer, R.M., Sutherland, J.W., *Proc.Roy.Soc.*, **A 237**, 1956, 439.
14. Barrer, R.M., Bultitude, F.W., Sutherland, J.W., *Trans. Faraday Soc.*, **53**, 1957, 1111.
15. Ruthven, D.M., Nature, *Phy.Sci.*, **70**, 1971, p. 232.